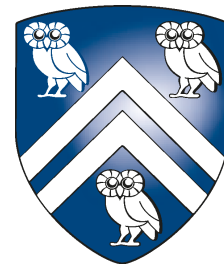


Gravitational Waves from Chiral Plasma Instability in the Standard Cosmology

Andrew J. Long
Rice University
@ ICTS workshop
Jan 1, 2025



RICE

Baryogenesis “by-products”

Among the outstanding problems in modern cosmology (dark matter, dark energy, inflation, baryogenesis) ... the matter / anti-matter asymmetry is uniquely challenging, because we only know **one number** ($n_B/s = 10^{-10}$)!

Therefore it is compelling to study models with “secondary predictions” that we can **test in the lab** (e.g., EWBG tested by collider observables & EDMs).

However, the physics of baryogenesis may not be within reach of terrestrial experiments (e.g., Affleck-Dine, GUT baryogenesis, high-scale leptogenesis).

In this case, we may still probe the origin of the matter / anti-matter asymmetry through observations of **baryogenesis “by-products”**.

Baryogenesis requires a departure from thermal equilibrium (Sakharov), and such conditions may create **additional cosmological relics** (e.g., gravity waves and topological defects) or the OOE conditions may be provided by other relics (e.g., primordial black holes and primordial magnetic fields).

If we could observe these other relics (**spectra**), we would gain a new handle on the origin of the matter / anti-matter asymmetry (**more numbers**).

Relic gravitational waves from the chiral plasma instability in the standard cosmological model

Axel Brandenburg^{1,2,3,4,†}, Emma Clarke^{4,*}, Tina Kahniashvili^{4,3,5,‡}, Andrew J. Long^{6,§} and Guotong Sun^{4,||}

¹*Nordita, KTH Royal Institute of Technology and Stockholm University, 10691 Stockholm, Sweden*

²*Department of Astronomy, AlbaNova University Center, Stockholm University, 10691 Stockholm, Sweden*

³*School of Natural Sciences and Medicine, Ilia State University, 0194 Tbilisi, Georgia*

⁴*McWilliams Center for Cosmology and Department of Physics, Carnegie Mellon University,
Pittsburgh, Pennsylvania 15213, USA*

⁵*Abastumani Astrophysical Observatory, Tbilisi, GE-0179, Georgia*

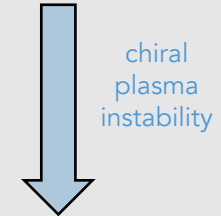
⁶*Department of Physics and Astronomy, Rice University, 6100 Main Street, Houston, Texas 77005, USA*

 (Received 19 July 2023; accepted 25 January 2024; published 27 February 2024)

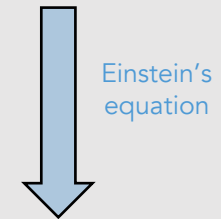
In the primordial plasma, at temperatures above the scale of electroweak symmetry breaking, the presence of chiral asymmetries is expected to induce the development of helical hypermagnetic fields through the phenomenon of chiral plasma instability. It results in magnetohydrodynamic turbulence due to the high conductivity and low viscosity and sources gravitational waves that survive in the universe today as a stochastic polarized gravitational wave background. In this article, we show that this scenario only relies on Standard Model physics, and therefore the observable signatures, namely the relic magnetic field and gravitational background, are linked to a single parameter controlling the initial chiral asymmetry. We estimate the magnetic field and gravitational wave spectra, and validate these estimates with 3D numerical simulations.

DOI: [10.1103/PhysRevD.109.043534](https://doi.org/10.1103/PhysRevD.109.043534)

initial particle asymmetry

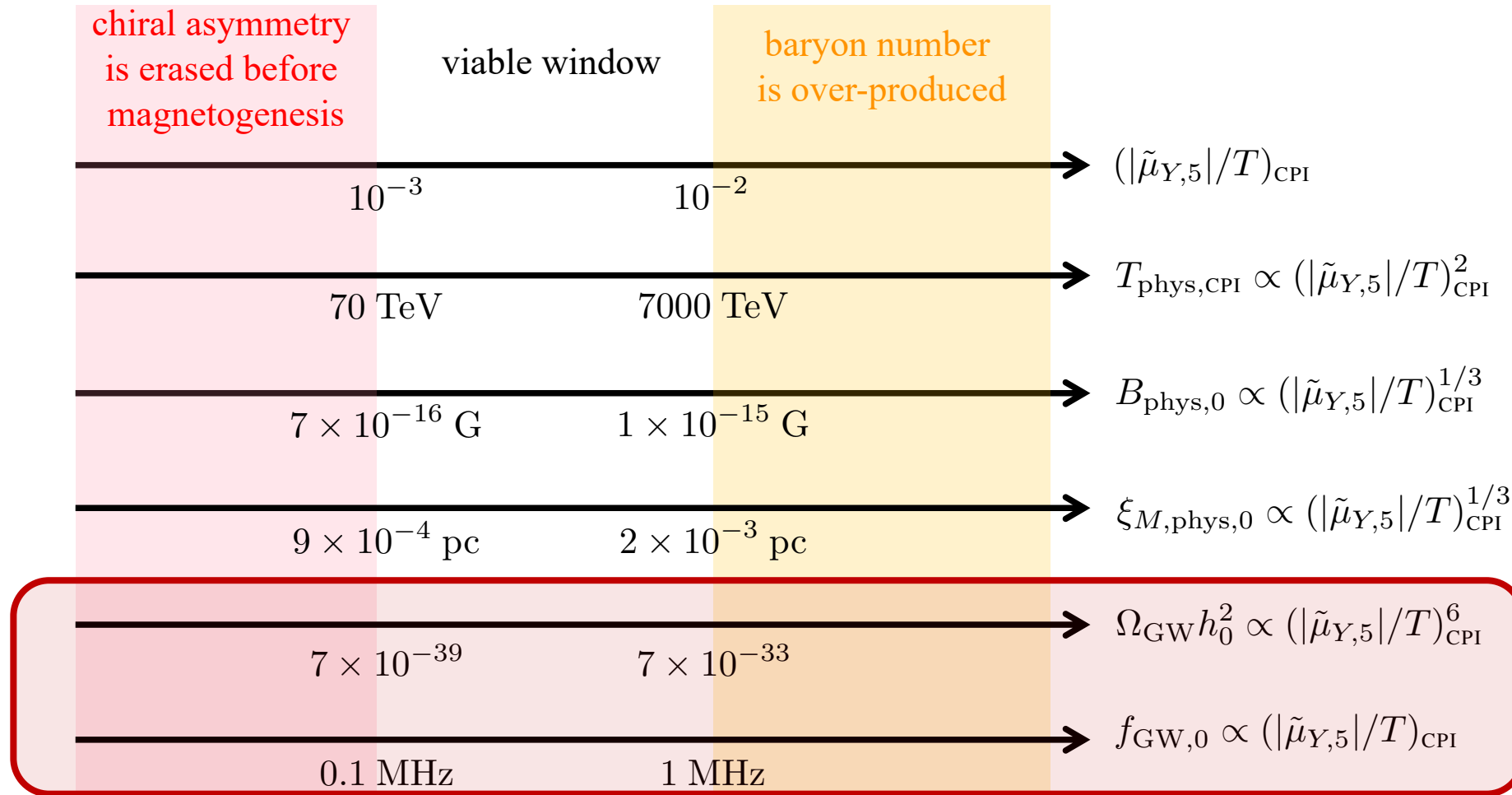


helical magnetic field



chiral grav-wave

where I'm going with this:



very high-frequency and very weak - not detectable

the electroweak plasma
& particle asymmetries

The electroweak plasma

We're thinking about the primordial plasma before the electroweak epoch.

FRW spacetime (homo / iso)

$$(ds)^2 = a(t)^2 [(dt)^2 - |d\mathbf{x}|^2]$$

$$H(t) = \frac{1}{a(t)} \frac{d}{dt} a(t)$$

R-dominated

$$\mathcal{E}(t) = \frac{\pi^2}{30} g_{*E}(t) T(t)^4$$

comoving entropy constant

$$s(t) = \frac{2\pi^2}{45} g_{*S}(t) T(t)^3 = \frac{2\pi^2}{45} g_{*S,0} T_0^3$$

at the electroweak epoch:

$$T_{\text{phys,ew}} \simeq 100 \text{ GeV}$$

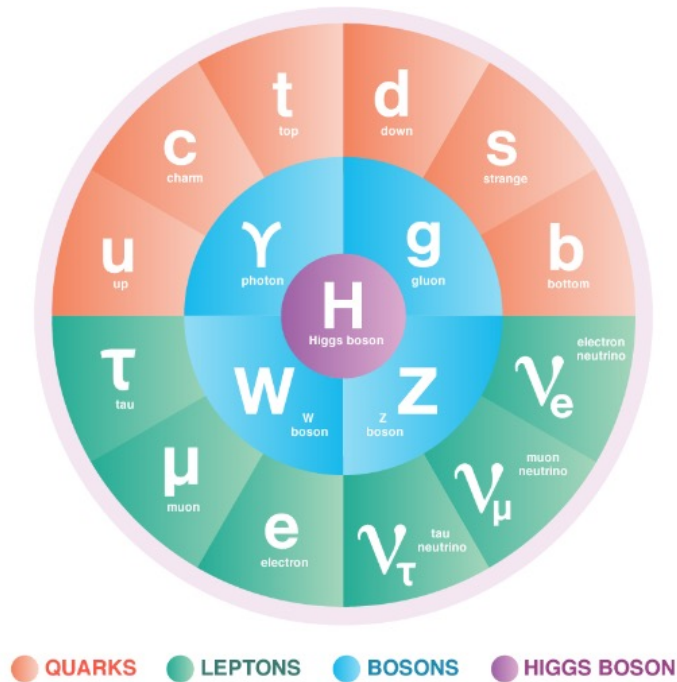
$$t_{\text{phys,ew}} \simeq (2.3 \times 10^{-11} \text{ sec}) \left(\frac{g_*}{106.75} \right)^{-1/2}$$

$$a_{\text{ew}} \simeq (7.8 \times 10^{-16} a_0) \left(\frac{g_*}{106.75} \right)^{-1/3}$$

$$d_{H,\text{phys,ew}} \simeq (1.4 \text{ cm}) \left(\frac{g_*}{106.75} \right)^{-1/2}$$

Particle content of the universe

The Standard Model of the Elementary Particles



electroweak unbroken phase

$$\langle \Phi \rangle = 0$$

$$\text{mass}(W^\pm, Z) = 0$$

$$\text{mass}(\text{quarks, leptons}) = 0$$

gauge theory

$$SU(3)_c \times SU(2)_L \times U(1)_Y$$

field content

$$Q = \begin{pmatrix} u_L \\ d_L \end{pmatrix} \sim (\mathbf{3}, \mathbf{2}, 1/3)$$

$$u_R \sim (\mathbf{3}, \mathbf{1}, 2/3)$$

$$d_R \sim (\mathbf{3}, \mathbf{1}, -1/3)$$

$$L = \begin{pmatrix} \nu_L \\ e_L \end{pmatrix} \sim (\mathbf{1}, \mathbf{2}, -1/2)$$

$$e_R \sim (\mathbf{1}, \mathbf{1}, -1)$$

$$G \sim (\mathbf{8}, \mathbf{1}, 0)$$

$$W \sim (\mathbf{1}, \mathbf{3}, 0)$$

$$B \sim (\mathbf{1}, \mathbf{1}, 0)$$

$$\Phi \sim (\mathbf{1}, \mathbf{2}, 1/2)$$

Particle asymmetries

All of the SM particles interact (scatter, decay, inverse-decay) & maintain thermal equilibrium

momentum distribution

$$dn_i(t) = g_i \frac{d^3\mathbf{p}}{(2\pi)^3} f_i(\mathbf{p}, t)$$
$$f_i(\mathbf{p}, t) = \begin{cases} (e^{[E_i(t) - \mu_i(t)]/T(t)} - 1)^{-1} \\ (e^{[E_i(t) - \mu_i(t)]/T(t)} + 1)^{-1} \end{cases}$$
$$E_i(t) = \sqrt{|\mathbf{p}|^2 + a(t)^2 m_i^2}$$

number density (for small μ_i)

$$n_i(t) = g_i \begin{cases} \frac{\zeta(3)}{\pi^2} T^3 + \frac{1}{6} \mu_i T^2 + O(\mu_i^2 T) \\ \frac{3}{4} \frac{\zeta(3)}{\pi^2} T^3 + \frac{1}{12} \mu_i T^2 + O(\mu_i^2 T) \end{cases}$$

if pair annihilation & production
are in thermal equilibrium:

$$\mu_i = -\mu_{\bar{i}}$$

particle asymmetries

$$\Delta n_i(t) = g_i \begin{cases} \frac{1}{3} \mu_i T^2 + O(\mu_i^2 T) \\ \frac{1}{6} \mu_i T^2 + O(\mu_i^2 T) \end{cases}$$

Standard Model Boltzmann Equations w/ Anomalous Sources

$$\frac{d\eta_{u_L^i}}{dx} = -\mathcal{S}_{UDW}^i - \sum_{j=1}^{N_g} \left(\mathcal{S}_{Uhu}^{ij} + \mathcal{S}_{Uu}^{ij} + \mathcal{S}_{Uhd}^{ij} \right) - \mathcal{S}_{s,\text{sph}} - \frac{N_c}{2} \mathcal{S}_{w,\text{sph}} + \left(N_c y_{Q_L}^2 \mathcal{S}_y^{\text{bkg}} + \frac{N_c}{2} \mathcal{S}_w^{\text{bkg}} + N_c \frac{y_{Q_L}}{2} \mathcal{S}_{yw}^{\text{bkg}} \right)$$

$$\frac{d\eta_{d_L^i}}{dx} = \mathcal{S}_{UDW}^i - \sum_{j=1}^{N_g} \left(\mathcal{S}_{Dhd}^{ij} + \mathcal{S}_{Dd}^{ij} + \mathcal{S}_{Dhu}^{ij} \right) - \mathcal{S}_{s,\text{sph}} - \frac{N_c}{2} \mathcal{S}_{w,\text{sph}} + \left(N_c y_{Q_L}^2 \mathcal{S}_y^{\text{bkg}} + \frac{N_c}{2} \mathcal{S}_w^{\text{bkg}} - N_c \frac{y_{Q_L}}{2} \mathcal{S}_{yw}^{\text{bkg}} \right)$$

$$\frac{d\eta_{\nu_L^i}}{dx} = -\mathcal{S}_{\nu EW}^i - \sum_{j=1}^{N_g} \mathcal{S}_{\nu he}^{ij} - \frac{1}{2} \mathcal{S}_{w,\text{sph}} + \left(y_{LL}^2 \mathcal{S}_y^{\text{bkg}} + \frac{1}{2} \mathcal{S}_w^{\text{bkg}} + \frac{y_{LL}}{2} \mathcal{S}_{yw}^{\text{bkg}} \right)$$

$$\frac{d\eta_{e_L^i}}{dx} = \mathcal{S}_{\nu EW}^i - \sum_{j=1}^{N_g} \left(\mathcal{S}_{Ehe}^{ij} + \mathcal{S}_{Ee}^{ij} \right) - \frac{1}{2} \mathcal{S}_{w,\text{sph}} + \left(y_{LL}^2 \mathcal{S}_y^{\text{bkg}} + \frac{1}{2} \mathcal{S}_w^{\text{bkg}} - \frac{y_{LL}}{2} \mathcal{S}_{yw}^{\text{bkg}} \right)$$

$$\frac{d\eta_{u_R^i}}{dx} = \sum_{j=1}^{N_g} \left(\mathcal{S}_{Uhu}^{ji} + \mathcal{S}_{Uu}^{ji} + \mathcal{S}_{Dhu}^{ji} \right) + \mathcal{S}_{s,\text{sph}} - N_c y_{u_R}^2 \mathcal{S}_y^{\text{bkg}}$$

$$\frac{d\eta_{d_R^i}}{dx} = \sum_{j=1}^{N_g} \left(\mathcal{S}_{Dhd}^{ji} + \mathcal{S}_{Dd}^{ji} + \mathcal{S}_{Uhd}^{ji} \right) + \mathcal{S}_{s,\text{sph}} - N_c y_{d_R}^2 \mathcal{S}_y^{\text{bkg}}$$

$$\frac{d\eta_{e_R^i}}{dx} = \sum_{j=1}^{N_g} \left(\mathcal{S}_{Ehe}^{ji} + \mathcal{S}_{Ee}^{ji} + \mathcal{S}_{\nu he}^{ji} \right) - y_{e_R}^2 \mathcal{S}_y^{\text{bkg}}$$

$$\frac{d\eta_{\phi^+}}{dx} = -\left(\mathcal{S}_{hhw} + \mathcal{S}_{hw} \right) + \sum_{i,j=1}^{N_g} \left(-\mathcal{S}_{Dhu}^{ij} + \mathcal{S}_{Uhd}^{ij} + \mathcal{S}_{\nu he}^{ij} \right)$$

$$\frac{d\eta_{\phi^0}}{dx} = \mathcal{S}_{hhw} - \mathcal{S}_h + \sum_{i,j=1}^{N_g} \left(-\mathcal{S}_{Uhu}^{ij} + \mathcal{S}_{Dhd}^{ij} + \mathcal{S}_{Ehe}^{ij} \right)$$

$$\frac{d\eta_{W^+}}{dx} = \left(\mathcal{S}_{hhw} + \mathcal{S}_{hw} \right) + \sum_{i=1}^{N_g} \left(\mathcal{S}_{UDW}^i + \mathcal{S}_{\nu EW}^i \right).$$

$$\mathcal{S}_{Dhu}^{ij} \equiv \frac{\gamma_{Dhu}^{ij}}{2} \left(\frac{\eta_{d_L^i}}{k_{d_L^i}} + \frac{\eta_{\phi^+}}{k_{\phi^+}} - \frac{\eta_{u_R^j}}{k_{u_R^j}} \right), \quad \mathcal{S}_{Uhu}^{ij} \equiv \frac{\gamma_{Uhu}^{ij}}{2} \left(\frac{\eta_{u_L^i}}{k_{u_L^i}} + \frac{\eta_{\phi^0}}{k_{\phi^0}} - \frac{\eta_{u_R^j}}{k_{u_R^j}} \right),$$

$$\mathcal{S}_{Uhd}^{ij} \equiv \frac{\gamma_{Uhd}^{ij}}{2} \left(\frac{\eta_{u_L^i}}{k_{u_L^i}} - \frac{\eta_{\phi^+}}{k_{\phi^+}} - \frac{\eta_{d_R^j}}{k_{d_R^j}} \right), \quad \mathcal{S}_{Dhd}^{ij} \equiv \frac{\gamma_{Dhd}^{ij}}{2} \left(\frac{\eta_{d_L^i}}{k_{d_L^i}} - \frac{\eta_{\phi^0}}{k_{\phi^0}} - \frac{\eta_{d_R^j}}{k_{d_R^j}} \right),$$

$$\mathcal{S}_{\nu he}^{ij} \equiv \frac{\gamma_{\nu he}^{ij}}{2} \left(\frac{\eta_{\nu_L^i}}{k_{\nu_L^i}} - \frac{\eta_{\phi^+}}{k_{\phi^+}} - \frac{\eta_{e_R^j}}{k_{e_R^j}} \right), \quad \mathcal{S}_{Ehe}^{ij} \equiv \frac{\gamma_{Ehe}^{ij}}{2} \left(\frac{\eta_{e_L^i}}{k_{e_L^i}} - \frac{\eta_{\phi^0}}{k_{\phi^0}} - \frac{\eta_{e_R^j}}{k_{e_R^j}} \right),$$

$$\mathcal{S}_{UDW}^i \equiv \gamma_{UDW}^i \left(\frac{\eta_{u_L^i}}{k_{u_L^i}} - \frac{\eta_{d_L^i}}{k_{d_L^i}} - \frac{\eta_{W^+}}{k_{W^+}} \right)$$

$$\mathcal{S}_{\nu EW}^i \equiv \gamma_{\nu EW}^i \left(\frac{\eta_{\nu_L^i}}{k_{\nu_L^i}} - \frac{\eta_{e_L^i}}{k_{e_L^i}} - \frac{\eta_{W^+}}{k_{W^+}} \right)$$

$$\mathcal{S}_{hhw} \equiv \gamma_{hhw} \left(\frac{\eta_{\phi^+}}{k_{\phi^+}} - \frac{\eta_{\phi^0}}{k_{\phi^0}} - \frac{\eta_{W^+}}{k_{W^+}} \right)$$

$$\mathcal{S}_{s,\text{sph}} \equiv \gamma_{s,\text{sph}} \sum_{i=1}^{N_g} \left(\frac{\eta_{u_L^i}}{k_{u_L^i}} + \frac{\eta_{d_L^i}}{k_{d_L^i}} - \frac{\eta_{u_R^i}}{k_{u_R^i}} - \frac{\eta_{d_R^i}}{k_{d_R^i}} \right),$$

$$\mathcal{S}_{w,\text{sph}} \equiv \gamma_{w,\text{sph}} \sum_{i=1}^{N_g} \left(\frac{N_c}{2} \frac{\eta_{u_L^i}}{k_{u_L^i}} + \frac{N_c}{2} \frac{\eta_{d_L^i}}{k_{d_L^i}} + \frac{1}{2} \frac{\eta_{\nu_L^i}}{k_{\nu_L^i}} + \frac{1}{2} \frac{\eta_{e_L^i}}{k_{e_L^i}} \right)$$

$$\mathcal{S}_y^{\text{bkg}} = \frac{1}{sT} \frac{\alpha_y}{4\pi} \frac{1}{2} \epsilon^{\mu\nu\rho\sigma} \langle Y_{\mu\nu} \rangle \langle Y_{\rho\sigma} \rangle$$

$$\mathcal{S}_w^{\text{bkg}} = \frac{1}{sT} \frac{1}{2} \frac{\alpha_w}{4\pi} \frac{1}{2} \epsilon^{\mu\nu\rho\sigma} \langle W_{\mu\nu}^a \rangle \langle W_{\rho\sigma}^a \rangle$$

$$\mathcal{S}_{yw}^{\text{bkg}} = \frac{1}{sT} \frac{gg'}{4\pi} \epsilon^{\mu\nu\rho\sigma} \langle Y_{\mu\nu} \rangle \langle W_{\rho\sigma}^3 \rangle.$$

$$\mathcal{S}_{Uu}^{ij} \equiv \gamma_{Uu}^{ij} \left(\frac{\eta_{u_L^i}}{k_{u_L^i}} - \frac{\eta_{u_R^j}}{k_{u_R^j}} \right),$$

$$\mathcal{S}_{Dd}^{ij} \equiv \gamma_{Dd}^{ij} \left(\frac{\eta_{d_L^i}}{k_{d_L^i}} - \frac{\eta_{d_R^j}}{k_{d_R^j}} \right),$$

$$\mathcal{S}_{Ee}^{ij} \equiv \gamma_{Ee}^{ij} \left(\frac{\eta_{e_L^i}}{k_{e_L^i}} - \frac{\eta_{e_R^j}}{k_{e_R^j}} \right),$$

$$\mathcal{S}_{hw} \equiv \gamma_{hw} \left(\frac{\eta_{\phi^+}}{k_{\phi^+}} - \frac{\eta_{W^+}}{k_{W^+}} \right)$$

$$\mathcal{S}_h \equiv \gamma_h \frac{\eta_{\phi^0}}{k_{\phi^0}}. \quad \eta = n/s$$

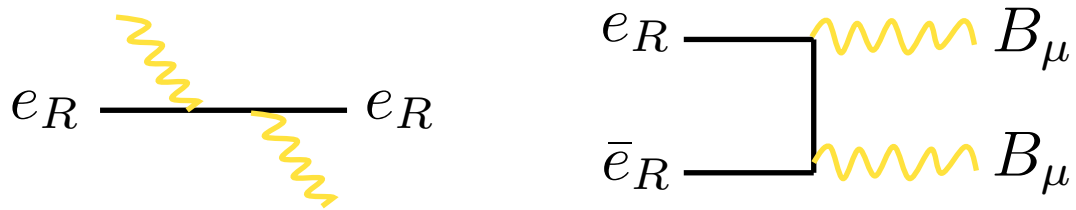
$$x = T/H \sim M_{\text{pl}}/T$$

$$k = \# \text{ degree of freedom}$$

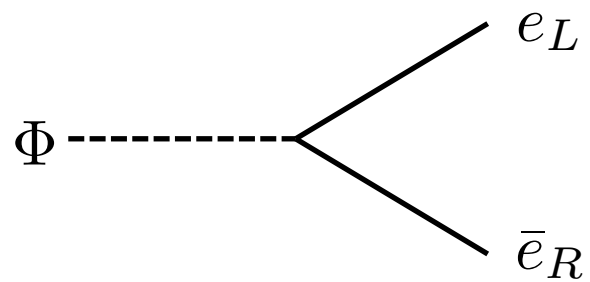
The special role of e_R

How does the asymmetry between e_R and $e_{\bar{R}}$ evolve?

The hypercharge interaction does not change the e_R asymmetry



But the Yukawa interactions do create / annihilate e_R



Can we “store” a chiral asymmetry in e_R ?

Chiral charge erasure

rate comes from: Bodeker & Schroder (2019)
see also: Cambbell, Davidson, Ellis, & Olive (1993)
Joyce & Shaposhnikov (1997)

The approximately conserved charges tend to be erased over time.

The limiting factor is the right-chiral electron, since it has $y_e \sim 3 \times 10^{-6}$.

chiral charge evolution

$$\frac{d}{dt} \mu_{e_R}(t) = -\Gamma_f(t) \mu_{e_R}(t)$$

interaction rate

$$\Gamma_f(t) \sim (1.3 \times 10^{-2}) y_e^2 T(t)$$

an exponential decay:

$$\mu_{e_R}(t) = \mu_{e_R,0} \exp \left[- \int_{t_0}^t dt' \Gamma_f(t') \right]$$

chiral-erasure epoch

$$T_{\text{phys},f} \simeq (80 \text{ TeV}) \left(\frac{g_*}{106.75} \right)^{-1/2}$$

$$t_{\text{phys},f} \simeq (3.7 \times 10^{-17} \text{ sec}) \left(\frac{g_*}{106.75} \right)^{1/2}$$

$$a_f \simeq (9.7 \times 10^{-19} a_0) \left(\frac{g_*}{106.75} \right)^{1/6}$$

$$d_{H,\text{phys},f} \simeq (2.2 \times 10^{-6} \text{ cm}) \left(\frac{g_*}{106.75} \right)^{1/2}$$

key message thus far

There might be a primordial chiral asymmetry (e.g., $e_R > \bar{e}_R$).

Yukawa interactions will erase the asymmetry once the plasma temperature drops to ~ 80 TeV.

If we want to do something fun with the chiral asymmetry,
we need to finish before $T = 80$ TeV
(or continue to source the asymmetry later)

magnetic field evolution
& chiral magnetic effect

A hypermagnetic field

mag screening in QCD: Gross, Pisarski, & Yaffe (1981)
 see also: Arnold, Son, & Yaffe (1996)

Where can we add magnetic fields to our primordial plasma?
 (for $T > 100$ GeV electroweak unbroken phase)

gauge interactions:

(1) electromagnetism is in here: $A_\mu = \cos \theta_W B_\mu + \sin \theta_W W_\mu^3$

$SU(3)_c \times SU(2)_L \times U(1)_Y$

(2) but non-Abelian magnetic fields are screened at finite temperature
 $m_{\text{mag}} \sim g^2 T$

(3) so the only place for long-range coherent magnetic fields is here
 $B_Y(\eta, \mathbf{x})$ and $E_Y(\eta, \mathbf{x})$

Evolution of hypermagnetic fields

conductivity: Arnold, Moore, & Yaffe (2000)

How do hypermagnetic fields evolve in the primordial plasma?

hyper-Maxwell equations

$$\nabla \cdot \mathbf{E}_Y = \rho_Y$$

$$\nabla \times \mathbf{E}_Y = -\frac{\partial}{\partial t} \mathbf{B}_Y$$

$$\nabla \cdot \mathbf{B}_Y = 0$$

$$\nabla \times \mathbf{B}_Y = \mathbf{J}_Y + \frac{\partial}{\partial t} \mathbf{E}_Y$$

continuity equation

$$\frac{\partial}{\partial \eta} \rho_Y + \nabla \cdot \mathbf{J}_Y = 0$$

constitutive relation

$$\mathbf{J}_Y = \underbrace{\sigma_Y (\mathbf{E}_Y + \mathbf{v} \times \mathbf{B}_Y)}_{\text{Ohm's Law}} + \underbrace{\frac{2}{\pi} \alpha_Y \mu_{Y,5} \mathbf{B}_Y}_{\text{chiral magnetic effect (CME)}}$$

Ohm's Law

chiral magnetic effect (CME)

fine structure constant

$$\alpha_Y = g'^2 / 4\pi \approx 1/100$$

conductivity

$$\sigma_Y \sim T / \alpha_Y \approx 100T$$

magnetic diffusivity

$$\eta_Y = 1 / \sigma_Y \approx 0.01T^{-1}$$

Chiral magnetic effect

Vilenkin (1980), Fukushima, Kharzeev, & Warringa (2008),
Aleksseev, Cheianov, & Frohlich (1998)
Boyarsky, Frohlich, & Ruchaiskiy (2011)

First studied for a relativistic electron-positron plasma in QED.

CME = in the presence of a chiral asymmetry, a magnetic field induces an electric current.

From the symmetry perspective, the CME could be correct.

$$\mathbf{J} \propto \mu_5 \mathbf{B}$$

mass dimensions: ✓

parity properties: ✓

\mathbf{J} = vector = P-odd

\mathbf{B} = axial-vector = P-even

m_e = scalar = P-even

μ_5 = pseudo-scalar = P-odd

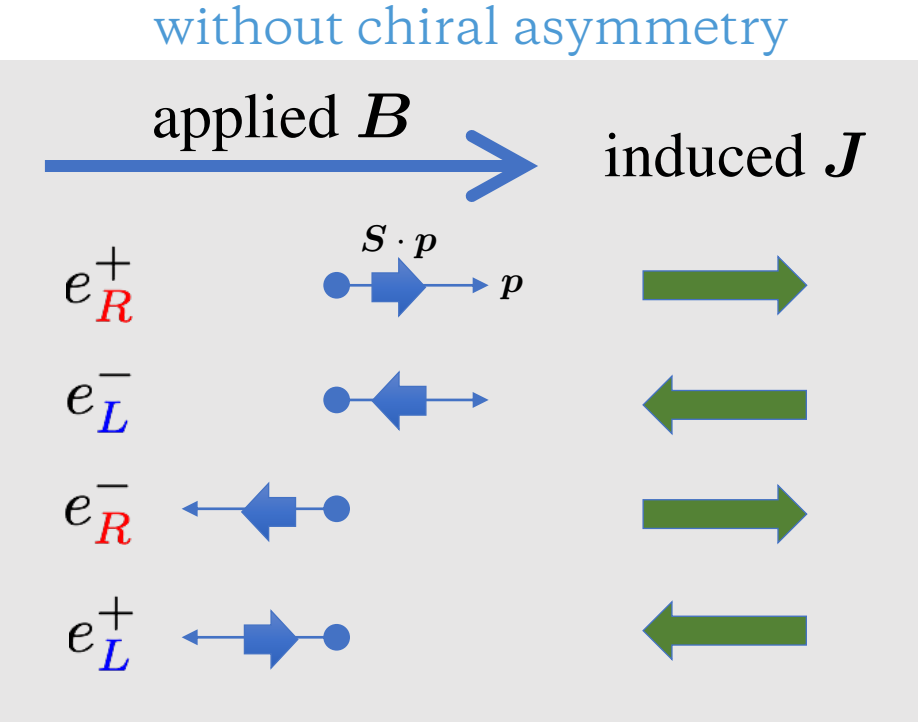
$\mu_5 \propto [\# \text{ R-chiral}] - [\# \text{ L-chiral}]$

Semiclassical understanding

Tashiro, Vachaspati, & Vilenkin (2012)

Consider, applying a B-field to a collection of (relativistic) electrons & positrons.

The magnetic dipole moment $\mu \sim qS$ wants to align with B ... the Hamiltonian is: $H = -\mu \cdot B$

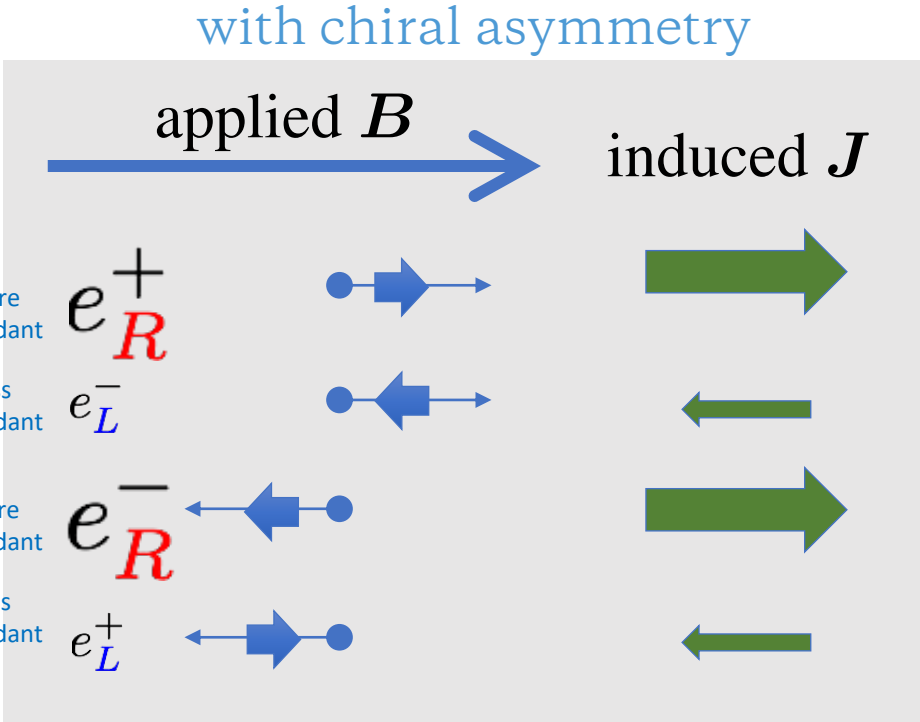
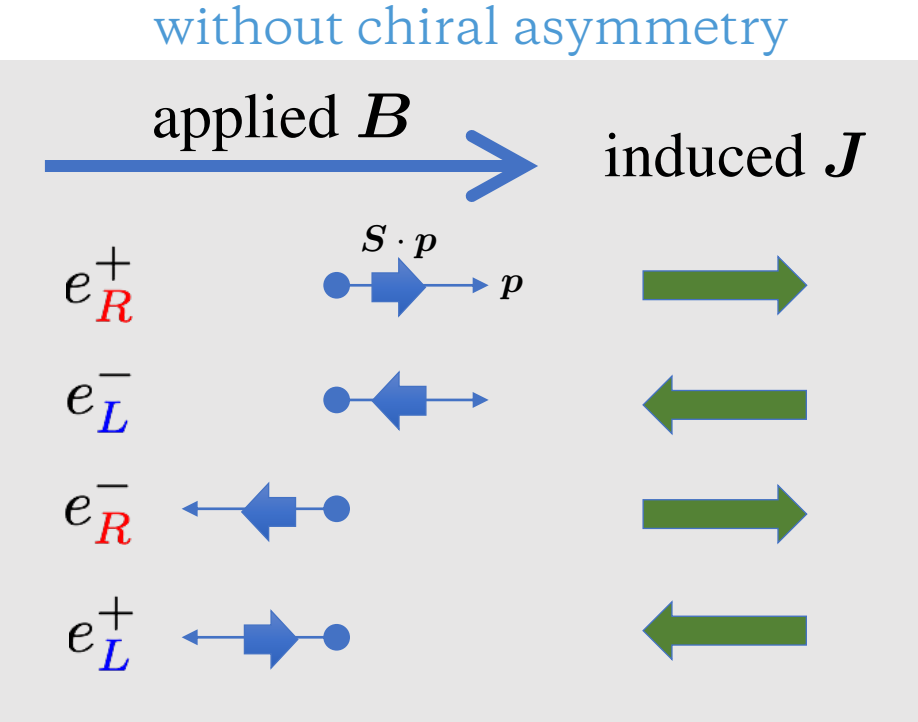


Semiclassical understanding

Tashiro, Vachaspati, & Vilenkin (2012)

Consider, applying a B-field to a collection of relativistic electrons & positrons.

The magnetic dipole moment $\mu \sim qS$ wants to align with B ... the Hamiltonian is: $H = -\mu \cdot B$



implies: $J \propto q^2 \mu_5 B$

CME recap

CME = in the presence of a chiral asymmetry, a magnetic field induces an electric current.

for electromagnetism: $\mathbf{J} = \frac{2}{\pi} \alpha \mu_5 \mathbf{B}$

for hypercharge: $\mathbf{J}_Y = \frac{2}{\pi} \alpha_Y \mu_{Y,5} \mathbf{B}_Y$

$$\mu_{Y,5}(t) = \sum_{\text{particles}} g_i \varepsilon_i Y_i^2 \mu_i(t)$$

$\varepsilon_i = \pm 1$ for R- and L-chiral particles

$Y_i =$ hypercharge of particle species i

magnetogenesis
via chiral plasma instability

Linearized field equations

similar equations of motion to axion inflation

Combining the hyper-Maxwell equations (and neglecting velocity v)

$$0 = \dot{\mathbf{B}}_Y - \eta_Y \nabla^2 \mathbf{B}_Y - \frac{2}{\pi} \alpha_Y \eta_Y \mu_{Y,5} \nabla \times \mathbf{B}_Y$$

Move to Fourier space (and assume homogenous μ_{Y5}).

Circular polarization modes decouple

$$0 = \dot{B}_{Y,k}^{(R)} + \eta_Y \left(k^2 - \text{sgn}(\mu_{Y,5}) k_{\text{CPI}} k \right) B_{Y,k}^{(R)}$$

$$0 = \dot{B}_{Y,k}^{(L)} + \eta_Y \left(k^2 + \text{sgn}(\mu_{Y,5}) k_{\text{CPI}} k \right) B_{Y,k}^{(L)}$$

where

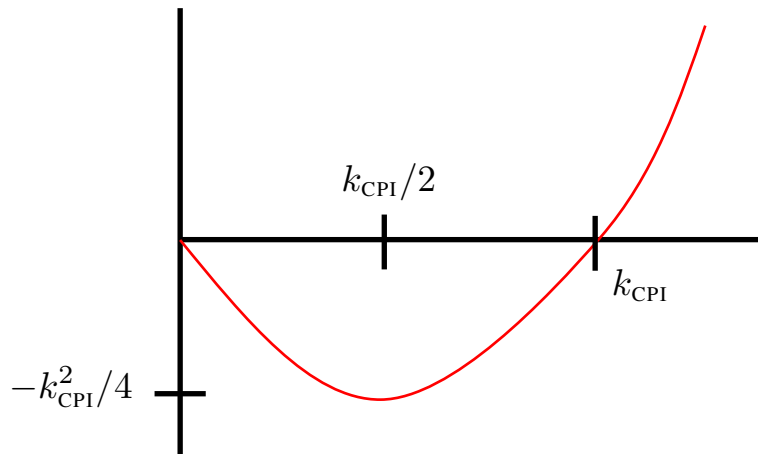
$$k_{\text{CPI}} = \frac{2}{\pi} \alpha_Y |\mu_{Y,5}|$$

Depending on the sign of μ_{Y5} , one mode or the other can be unstable.

Chiral plasma instability

Explore the dependence on wavenumber

$$0 = \dot{B}_{Y,k}^{(R)} + \eta_Y \left(k^2 - k_{\text{CPI}} k \right) B_{Y,k}^{(R)}$$



- modes with $k > k_{\text{CPI}}$ are decaying (Ohmic dissipation)
- modes with $k < k_{\text{CPI}}$ have a tachyonic instability
- modes with $k = k_{\text{CPI}}/2$ grow fastest

$$B_{Y,k}^{(R)}(t) \propto \exp \left[\frac{1}{4} \eta_Y k_{\text{CPI}}^2 t \right]$$

- typically k_{CPI} is deep inside the horizon

CPI = tachyonic growth of a helical magnetic field due to the CME

Helicity saturation

Since either the R- or L-polarized modes grow, the resultant magnetic field is helical.

As the helicity grows, the chiral asymmetry is depleted:

$$\partial_\mu j_{Y,5}^\mu \sim -\frac{g'^2}{16\pi^2} Y_{\mu\nu} \tilde{Y}^{\mu\nu} \quad \Rightarrow \quad \frac{\partial}{\partial t} n_{Y,5} \sim -\frac{1}{\pi} \alpha_Y \frac{\partial}{\partial t} \mathcal{H}_M$$

The exponential growth must saturate when the initial asymmetry is 'used up'

helicity density: $\mathcal{H}_{M,\text{CPI}} \sim \frac{\pi}{6} \frac{1}{\alpha_Y} |\mu_{Y,5}| T_{\text{CPI}}^2$

coherence length: $\xi_{M,\text{CPI}} \approx 2\pi / (k_{\text{CPI}}/2)$

field strength: $B_{\text{CPI}} \approx \sqrt{\mathcal{H}_{M,\text{CPI}} / \xi_{M,\text{CPI}}}$

(We will validate these estimates using MHD simulations.)

using
 $n_{Y,5} = \frac{1}{6} \mu_{Y,5} T^2$
 $Y\tilde{Y} = -4\mathbf{E}_Y \cdot \mathbf{B}_Y = 4\frac{\partial}{\partial t}(\mathbf{A}_Y \cdot \mathbf{B}_Y) + \dots$

Magnetogenesis

Typical scales

$$\begin{aligned}a_{\text{CPI}} &\simeq (1.1 \times 10^{-18} a_0) \left(\frac{g_*}{106.75}\right)^{1/6} \left(\frac{\eta_Y}{0.01 T^{-1}}\right)^{-1} \left(\frac{|\mu_{Y,5}|/T}{10^{-3}}\right)^{-2} \\T_{\text{phys,CPI}} &\simeq (7.2 \times 10^4 \text{ GeV}) \left(\frac{g_*}{106.75}\right)^{-1/2} \left(\frac{\eta_Y}{0.01 T^{-1}}\right) \left(\frac{|\mu_{Y,5}|/T}{10^{-3}}\right)^2 \\d_{H,\text{CPI}} &\simeq (2.5 \times 10^{12} \text{ cm } a_0^{-1}) \left(\frac{g_*}{106.75}\right)^{1/3} \left(\frac{\eta_Y}{0.01 T^{-1}}\right)^{-1} \left(\frac{|\mu_{Y,5}|/T}{10^{-3}}\right)^{-2} \\\xi_{M,\text{CPI}} &\simeq (5.0 \times 10^5 \text{ cm } a_0^{-1}) \left(\frac{g_*}{106.75}\right)^{1/3} \left(\frac{|\mu_{Y,5}|/T}{10^{-3}}\right)^{-1} \\B_{\text{CPI}} &\simeq (5.0 \times 10^{-11} \text{ G } a_0^2) \left(\frac{g_*}{106.75}\right)^{-2/3} \left(\frac{|\mu_{Y,5}|/T}{10^{-3}}\right) \\\Omega_{B,\text{CPI}} &\simeq (3.8 \times 10^{-10}) \left(\frac{g_*}{106.75}\right)^{-1} \left(\frac{|\mu_{Y,5}|/T}{10^{-3}}\right)^2\end{aligned}$$

If $\mu_{Y5}/T > \sim 10^{-3}$ then the CPI develops before chiral charge erasure.

Inverse cascade

A maximally-helical field co-evolves with the plasma subject to the turbulent inverse-cascade:

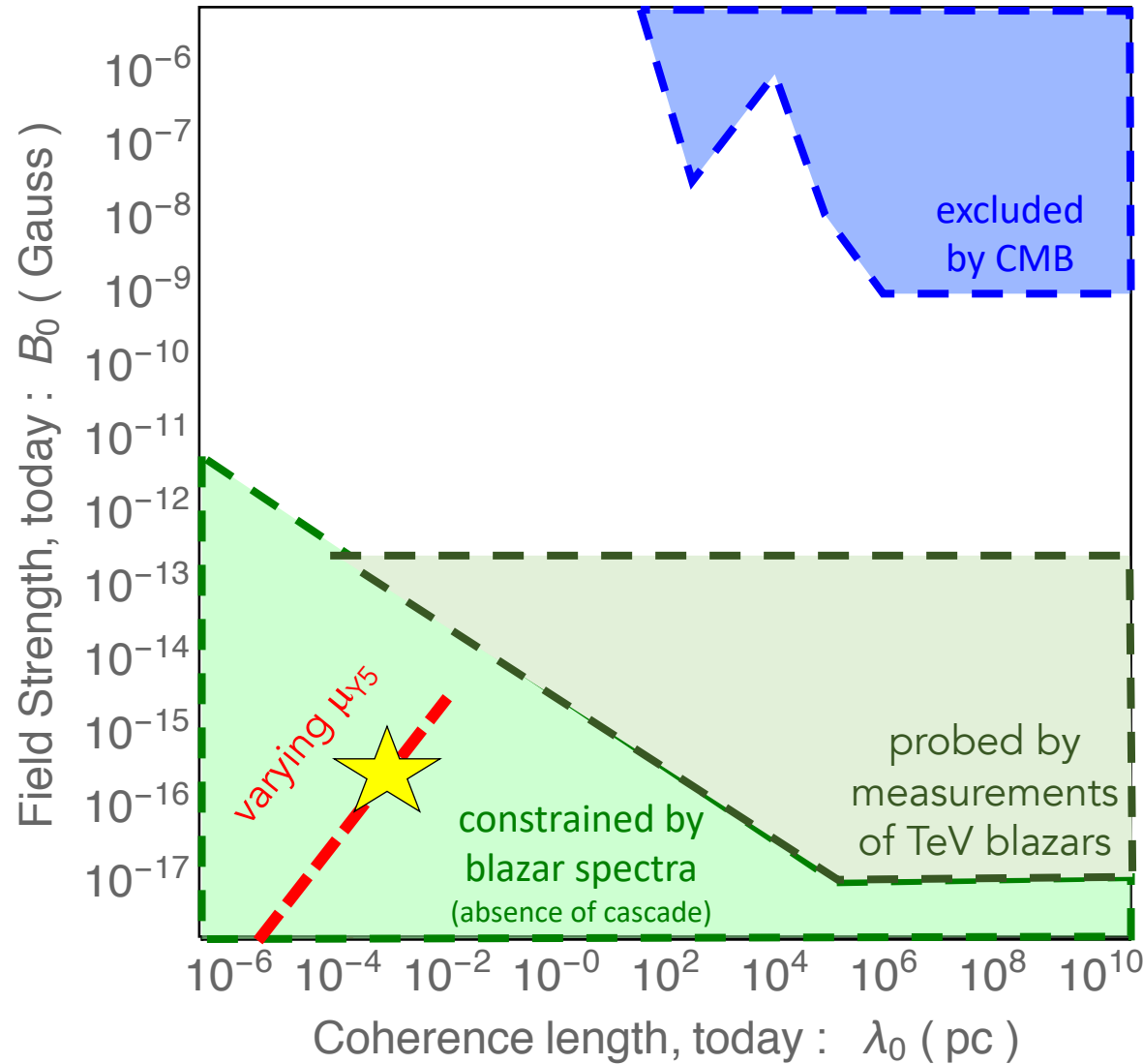
$$B_0 = B_{\text{CPI}} \left(\frac{t_{\text{rec}}}{t_{\text{CPI}}} \right)^{-1/3} \quad \text{and} \quad \xi_{B,0} = \xi_{B,\text{CPI}} \left(\frac{t_{\text{rec}}}{t_{\text{CPI}}} \right)^{2/3} \quad \text{so} \quad \mathcal{H}_{B,0} = \mathcal{H}_{B,\text{CPI}}$$

The field today is expected to be

$$\xi_{M,\text{phys},0} \simeq (9.5 \times 10^{-4} \text{ pc}) \left(\frac{g_*}{106.75} \right)^{1/9} \left(\frac{\eta_Y}{0.01 T^{-1}} \right)^{2/3} \left(\frac{|\mu_{Y,5}|/T}{10^{-3}} \right)^{1/3}$$
$$B_{\text{phys},0} \simeq (6.6 \times 10^{-16} \text{ G}) \left(\frac{g_*}{106.75} \right)^{-5/9} \left(\frac{\eta_Y}{0.01 T^{-1}} \right)^{-1/3} \left(\frac{|\mu_{Y,5}|/T}{10^{-3}} \right)^{1/3}$$

IGMF parameter space

adapted from: Durrer & Neronov (2013)



The relic of the primordial magnetic field is an intergalactic magnetic field today

$$\xi_{M,\text{phys},0} \simeq (9.5 \times 10^{-4} \text{ pc}) \left(\frac{|\mu_{Y,5}|/T}{10^{-3}} \right)^{1/3}$$

$$B_{\text{phys},0} \simeq (6.6 \times 10^{-16} \text{ G}) \left(\frac{|\mu_{Y,5}|/T}{10^{-3}} \right)^{1/3}$$

- too weak to explain blazars
- too weak to seed galactic B-field

grav-wave generation
& stochastic GW background

Einstein's equation

for details: Roper Pol, Brandenburg, Kahniashvili, Kosowsky, & Mandal (2018)

The primordial magnetic field sources gravitational wave radiation

$$G_{\mu\nu} = 8\pi G T_{\mu\nu}$$

$$\partial_t^2 h_{ij} - \nabla^2 h_{ij} = 16\pi G T_{ij}$$

$$T_{ij} \sim B_i B_j \quad (\text{transverse / traceless part})$$

$$\mathcal{E}_{\text{gw}} = \langle \partial_t h_{ij} \partial_t h_{ij} \rangle / (32\pi G)$$

parametrically:

$$h \sim (GB^2)/\xi^2$$
$$\mathcal{E}_{\text{gw}} \sim \xi^2 h^2 / G \sim G\xi^2 B^4$$

GW estimates

At the time of production

$$f_{\text{gw,CPI}} \approx 2/\xi_{M,\text{CPI}}$$

$$\mathcal{E}_{\text{gw,CPI}} \sim (G/2\pi) a_{\text{CPI}}^{-2} \xi_{M,\text{CPI}}^2 B_{\text{CPI}}^4$$

there's a 2 because the source
is quadratic in the field

Frequency and cosmological energy fraction of stochastic GW today:

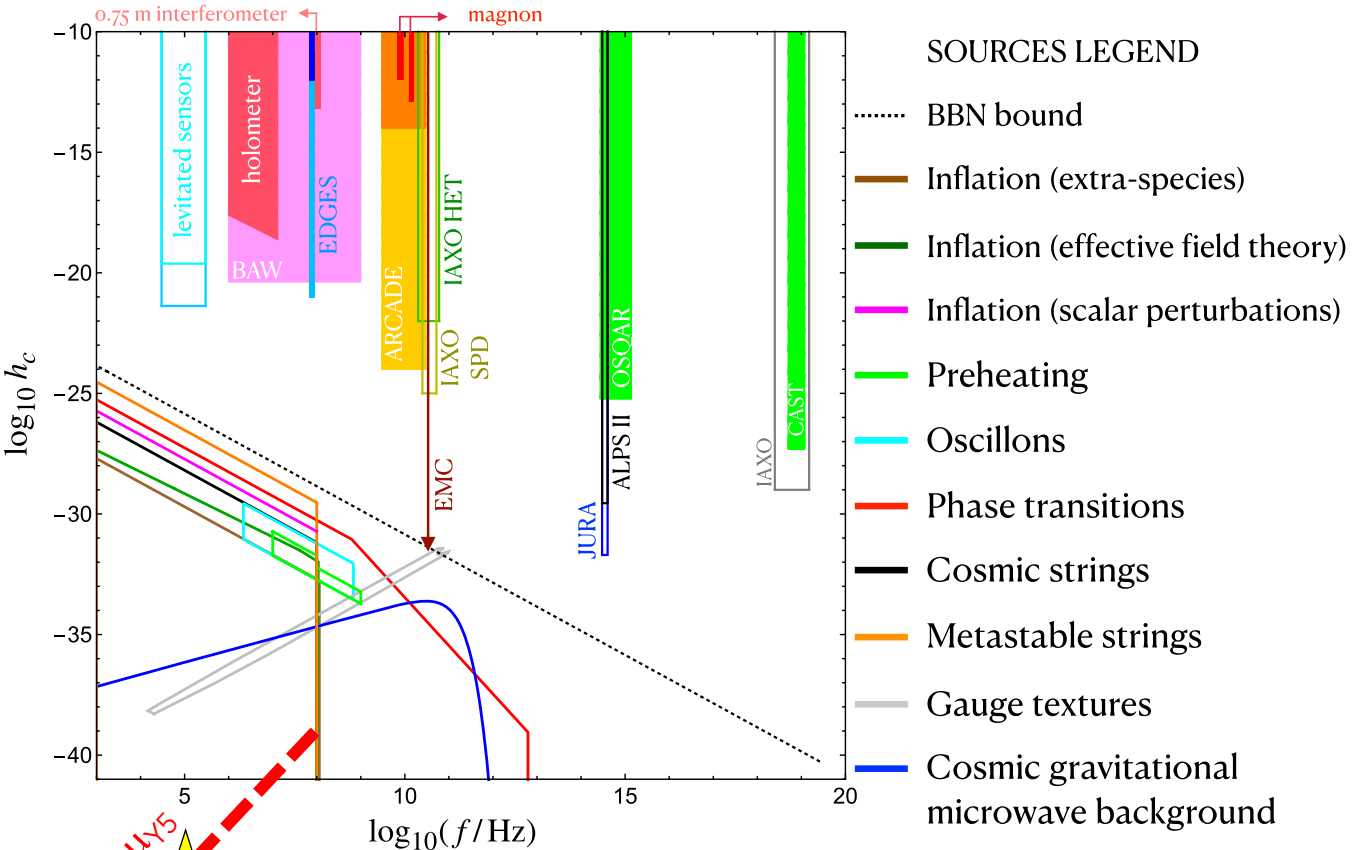
$$f_{\text{gw,phys},0} = (1 \times 10^5 \text{ Hz}) \left(\frac{|\mu_{Y,5}|/T}{10^{-3}} \right)$$

$$(\Omega_{\text{gw}} h^2)_0 = (7 \times 10^{-39}) \left(\frac{\eta_Y}{0.01 T^{-1}} \right)^2 \left(\frac{|\mu_{Y,5}|/T}{10^{-3}} \right)^6$$

The GW signal is **high-frequency** and **very low amplitude** (even for $\mu_{Y5}/T = 1$)

Searches for high-freq grav waves

review on high-freq grav wave: Aggarwal et al (2021)



$$f_{\text{gw},0} = (1 \times 10^5 \text{ Hz}) \left(\frac{|\mu_{Y,5}|/T}{10^{-3}} \right)$$

$$(\Omega_{\text{gw}} h^2)_0 = (7 \times 10^{-39}) \left(\frac{|\mu_{Y,5}|/T}{10^{-3}} \right)^6$$

$$h_c = (1 \times 10^{-45}) \left(\frac{|\mu_{Y,5}|/T}{10^{-3}} \right)^2$$

using

$$\Omega_{\text{gw}} = \frac{\pi f^2 h_c^2}{4G\mathcal{E}_{\text{cr}}}$$

numerical validation
with PENCIL CODE sims

MHD equations + CME

Fully nonlinear system of equations

$$\frac{\partial \mathbf{A}}{\partial t} = \mathbf{u} \times \mathbf{B} + \eta(\mu_5 \mathbf{B} - \mathbf{J}), \quad (5)$$

$$\frac{\partial \mu_5}{\partial t} = -\nabla \cdot (\mu_5 \mathbf{u}) - \lambda \eta (\mu_5 \mathbf{B} - \mathbf{J}) \cdot \mathbf{B} + D_5 \nabla^2 \mu_5, \quad (6)$$

$$\begin{aligned} \frac{D\mathbf{u}}{Dt} = & \frac{2}{\rho} \nabla \cdot (\rho \nu \mathbf{S}) - \frac{1}{4} \nabla \ln \rho + \frac{\mathbf{u}}{3} (\nabla \cdot \mathbf{u} + \mathbf{u} \cdot \nabla \ln \rho) \\ & - \frac{\mathbf{u}}{\rho} [\mathbf{u} \cdot (\mathbf{J} \times \mathbf{B}) + \eta \mathbf{J}^2] + \frac{3}{4\rho} \mathbf{J} \times \mathbf{B}, \end{aligned} \quad (7)$$

$$\begin{aligned} \frac{\partial \ln \rho}{\partial t} = & -\frac{4}{3} (\nabla \cdot \mathbf{u} + \mathbf{u} \cdot \nabla \ln \rho) \\ & + \frac{1}{\rho} [\mathbf{u} \cdot (\mathbf{J} \times \mathbf{B}) + \eta \mathbf{J}^2], \end{aligned} \quad (8)$$

$$\mathbf{S}_{ij} = (\partial_j u_i + \partial_i u_j)/2 - \delta_{ij} \nabla \cdot \mathbf{u}/3$$

$$\frac{\partial^2}{\partial t^2} \tilde{h}_{+/\times}(\mathbf{k}, t) + k^2 \tilde{h}_{+/\times}(\mathbf{k}, t) = \frac{6 H_*}{t \mathcal{E}_{\text{cr}}} \tilde{T}_{+/\times}(\mathbf{k}, t),$$

magnetic diffusivity η

kinematic viscosity ν

chiral diffusion coeff. D_5

rescaled chem. pot. μ_5

chiral depletion param. λ

PENCIL CODE

parallelized

6th order finite differences

3rd order time-stepping

1024³ mesh points

initially: weak seed field,

vanishing plasma velocity,

homogenous chem. pot.

Parameters

cf, Brandenburg, He, Kahnishvili, Rheinhardt, & Schober (2021)

Dynamic range issues prevent studying the “expected” parameters.

| Run | ηH_* | $(\mathcal{E}_{\text{cr}} \lambda)^{1/2}/H_*$ | μ_{50}/H_* | v_μ | v_λ | $\eta \mu_{50}^2/H_*$ | k_1/H_* | $\mathcal{E}_M^{\text{max}}/\mathcal{E}_{\text{cr}}$ | $\mathcal{E}_{\text{GW}}^{\text{sat}}/\mathcal{E}_{\text{cr}}$ | q |
|----------|---------------------|---|-----------------------|---------------------------------|--------------------------|-----------------------|-----------------|--|--|-------|
| B1 | 1×10^{-6} | 2×10^4 | 10^4 | 1×10^{-2} | 5×10^{-1} | 1×10^2 | 1×10^2 | 1.6×10^{-2} | 4.7×10^{-12} | 0.027 |
| B10 | 1×10^{-3} | 2×10^4 | 10^4 | 1×10^1 | 5×10^{-1} | 1×10^5 | 1×10^2 | 6.0×10^{-2} | 6.0×10^{-9} | 12 |
| A1 | 1×10^{-6} | 5×10^4 | 10^4 | 1×10^{-2} | 2×10^{-1} | 1×10^2 | 1×10^2 | 4.6×10^{-3} | 8.9×10^{-14} | 0.032 |
| A12 | 5×10^{-3} | 5×10^4 | 10^4 | 5×10^1 | 2×10^{-1} | 5×10^5 | 5×10^1 | 9.2×10^{-3} | 3.0×10^{-10} | 18 |
| X1 | 5×10^{-8} | 10^{10} | 10^6 | 5×10^{-2} | 1×10^{-4} | 5×10^4 | 5×10^3 | 2.4×10^{-9} | 8.8×10^{-31} | 0.39 |
| X2 | 5×10^{-9} | 10^{10} | 10^6 | 5×10^{-3} | 1×10^{-4} | 5×10^3 | 5×10^3 | 2.4×10^{-9} | 1.6×10^{-30} | 0.53 |
| X3 | 5×10^{-10} | 10^{10} | 10^6 | 5×10^{-4} | 1×10^{-4} | 5×10^2 | 5×10^3 | 2.4×10^{-9} | 1.1×10^{-30} | 0.44 |
| X4 | 5×10^{-11} | 10^{10} | 10^6 | 5×10^{-5} | 1×10^{-4} | 5×10^1 | 5×10^3 | 2.3×10^{-9} | 3.1×10^{-31} | 0.12 |
| Y1 | 5×10^{-8} | 7×10^{11} | 10^6 | 5×10^{-2} | 1×10^{-6} | 5×10^4 | 5×10^3 | 4.9×10^{-13} | 3.6×10^{-38} | 0.39 |
| Y2 | 5×10^{-8} | 7×10^{11} | 10^6 | 5×10^{-2} | 1×10^{-6} | 5×10^4 | 2×10^3 | 4.4×10^{-13} | 3.2×10^{-37} | 1.3 |
| Y3 | 5×10^{-8} | 7×10^{11} | 10^6 | 5×10^{-2} | 1×10^{-6} | 5×10^4 | 1×10^3 | 3.3×10^{-13} | 6.9×10^{-37} | 2.5 |
| expected | $10^{-15} \eta_2$ | 6×10^{12} | $5 \times 10^7 \mu_3$ | $6 \times 10^{-8} \eta_2 \mu_3$ | $8 \times 10^{-6} \mu_3$ | $3 \eta_2 \mu_3^2$ | — | $6 \times 10^{-15} \mu_3^2$ | $7 \times 10^{-39} \eta_2^2 \mu_3^6$ | — |

$$v_\mu = \mu_{50} \eta$$

$$v_\lambda = \mu_{50} / (\mathcal{E}_{\text{cr}} \lambda)^{1/2}$$

$$\mu_{50} = 2\alpha_Y \tilde{\mu}_{Y,5} / \pi$$

$$\lambda = 192\alpha_Y^2 / T^2$$

$$D_5 = \nu = \eta = 1/\sigma$$

$$\eta_2 = \eta_Y / (0.01 T^{-1})$$

$$\mu_3 = \tilde{\mu}_{Y,5} / (10^{-3} T)$$

Spectra for PMF and GWs

- $tH_* = 5.37$ (green-dashed)
- $tH_* = 3.66$ (blue-dashed)
- $tH_* = 2.98$ (solid)
- $tH_* = 2.71$ (orange-dot)
- $tH_* = 2.56$ (red-dot)
- $tH_* = 2.41$ (black-dot)

NB : $\mathcal{E}_M(\mathbf{x}, t) = \frac{1}{2} \langle |\mathbf{B}(\mathbf{x}, t)|^2 \rangle = \int \frac{d^3\mathbf{k}}{(2\pi)^3} P_B(\mathbf{k}) = \int \frac{dk}{k} \underbrace{\frac{k^3}{2\pi^2} P_B(k)}_{= d\mathcal{E}_M/d \ln k} = \int dk E_M(k)$

- mag energy grows at $k_{\text{CPI}}/2$
- GW energy grows while mag energy grows
- mag energy reaches maximum and GW energy spectrum saturates (solid curves)
- subsequently mag energy evolves with the inverse cascade scaling (expected for helical):

$$B \propto t^{-1/3} \quad \text{so} \quad \mathcal{E}_M \propto t^{-2/3}$$

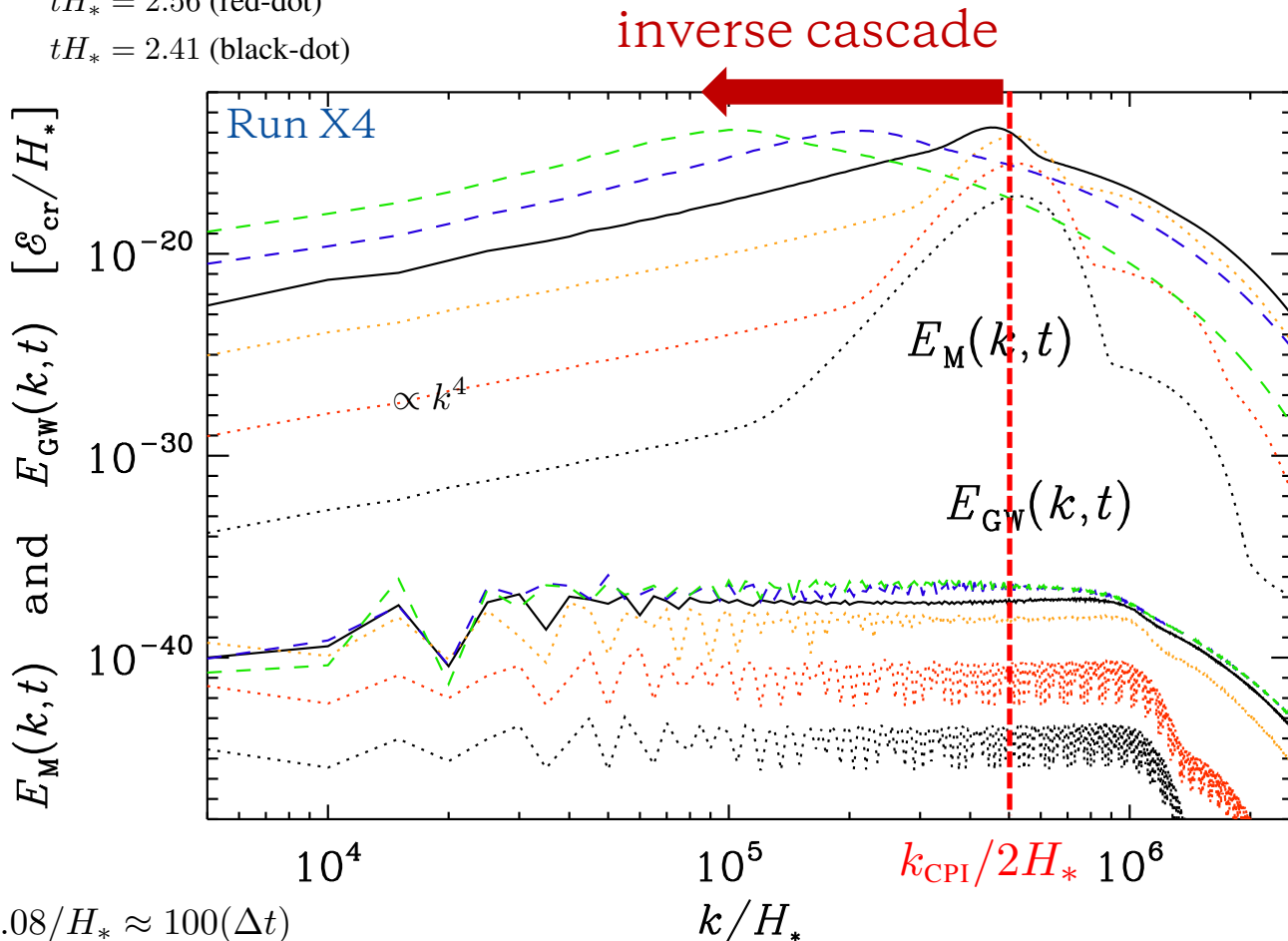
$$\xi_M \propto t^{2/3} \quad \text{so} \quad k_M \propto t^{-2/3}$$

$$E_M \sim \mathcal{E}_M/k_M \propto t^0$$

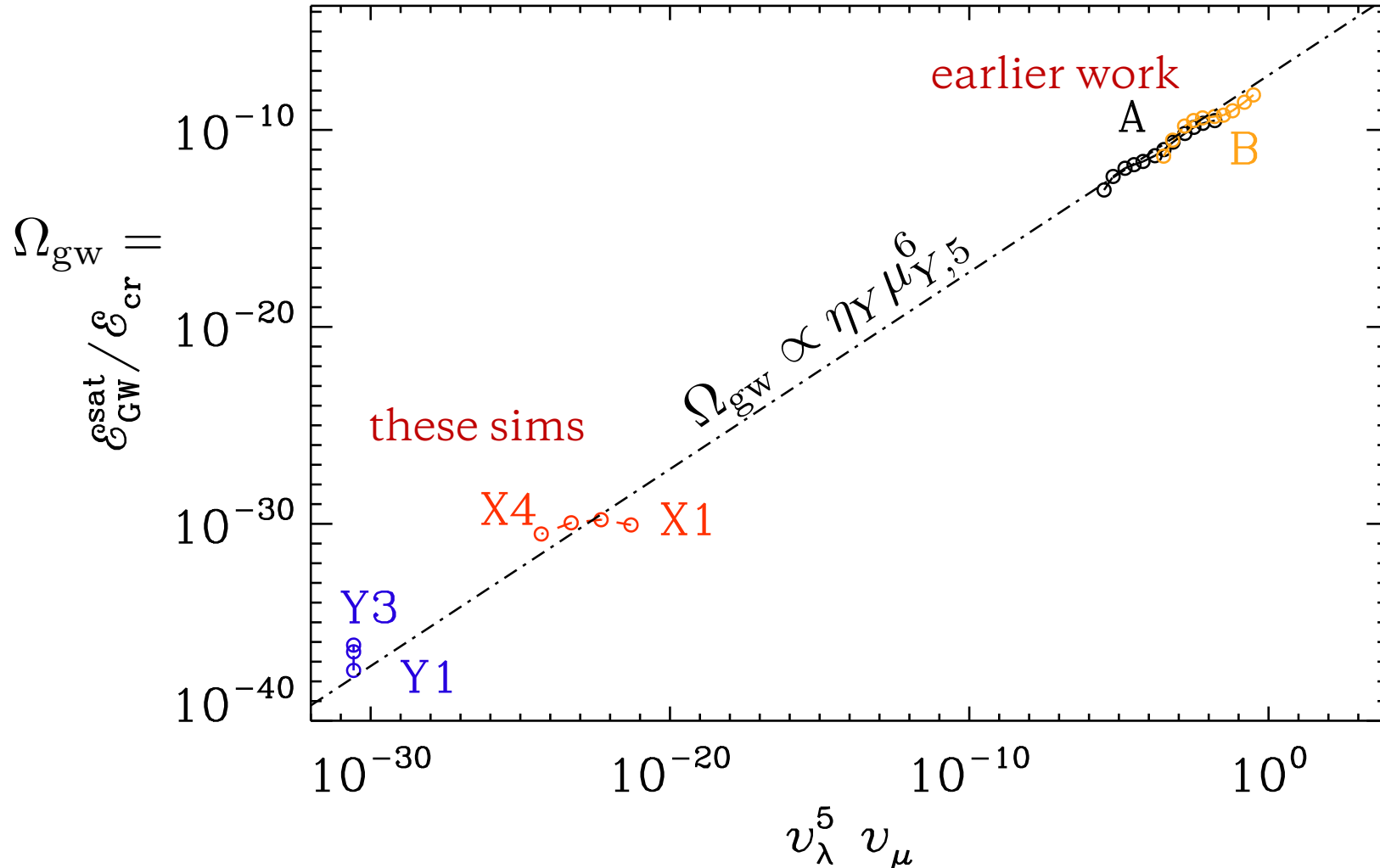
- resultant GW energy spectrum is blue-tilted

$$\frac{d\mathcal{E}_{\text{gw}}}{d \ln k} = k E_{\text{GW}} \propto k^1 \quad (k \lesssim k_{\text{CPI}})$$

- (scaling should extend down to $k_{\text{IR}} \sim H$)
- (most energy at $k_{\text{UV}} \sim k_{\text{CPI}}$)



Comparison w/ previous studies



Earlier work studied GW from CME at the EW epoch, assuming no chiral asymmetry washout (see Run Series A & B)

We explore parameters that are closer to the expectation for early universe cosmology at $T > 80$ TeV (see Run Series X and Y)

Main difference is the choice of magnetic diffusivity: η_Y . (see the table on prev. slide)

For those parameters, the GW signal is found to be weaker.

Scaling with $v_\lambda^5 v_\mu$ from earlier work, confirmed over wider range.

B-number overproduction & an upper bound on μ_{Y5}

Sourcing baryon number

Fujita & Kamada (2016), Kamada & AL (2016a,b),
Jimenez, Kamada, Schmitz, Xu (2017)
see also: Giovannini & Shaposhnikov
(also gravitational anomaly: cf, Evangelos's talk)

Varying hypermagnetic helicity sources B and L-number

$$\partial_\mu j_B^\mu = \partial_\mu j_L^\mu = 3 \frac{g^2}{16\pi^2} W^a \tilde{W}^a - 3 \frac{g'^2}{16\pi^2} Y \tilde{Y}$$
$$\dot{n}_B = \dot{n}_L = -3 \frac{g'^2}{4\pi^2} \dot{\mathcal{H}}_Y + \dots$$

At the EW crossover, there is a change in helicity when the B_Y field converts to B_{em}

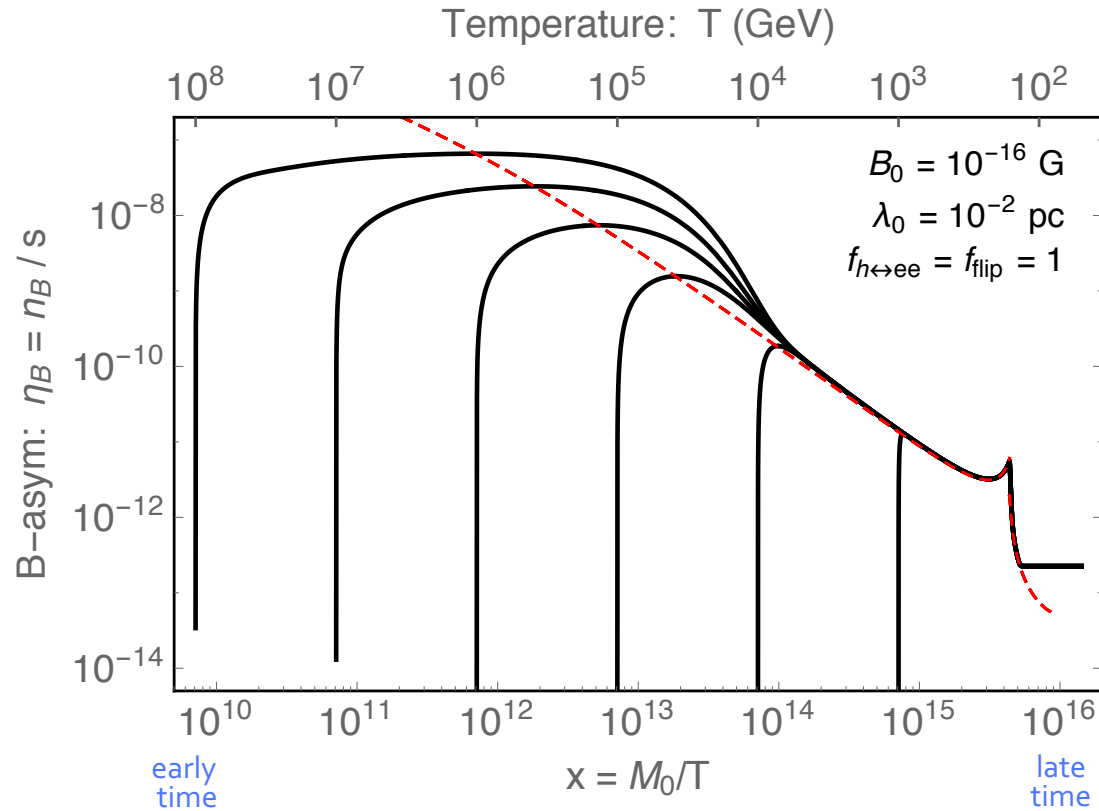
- this could explain the matter/antimatter asymmetry!
- but it would be a problem if too many baryons are created

(B+L) washout is avoided

Kamada & AL (2016)

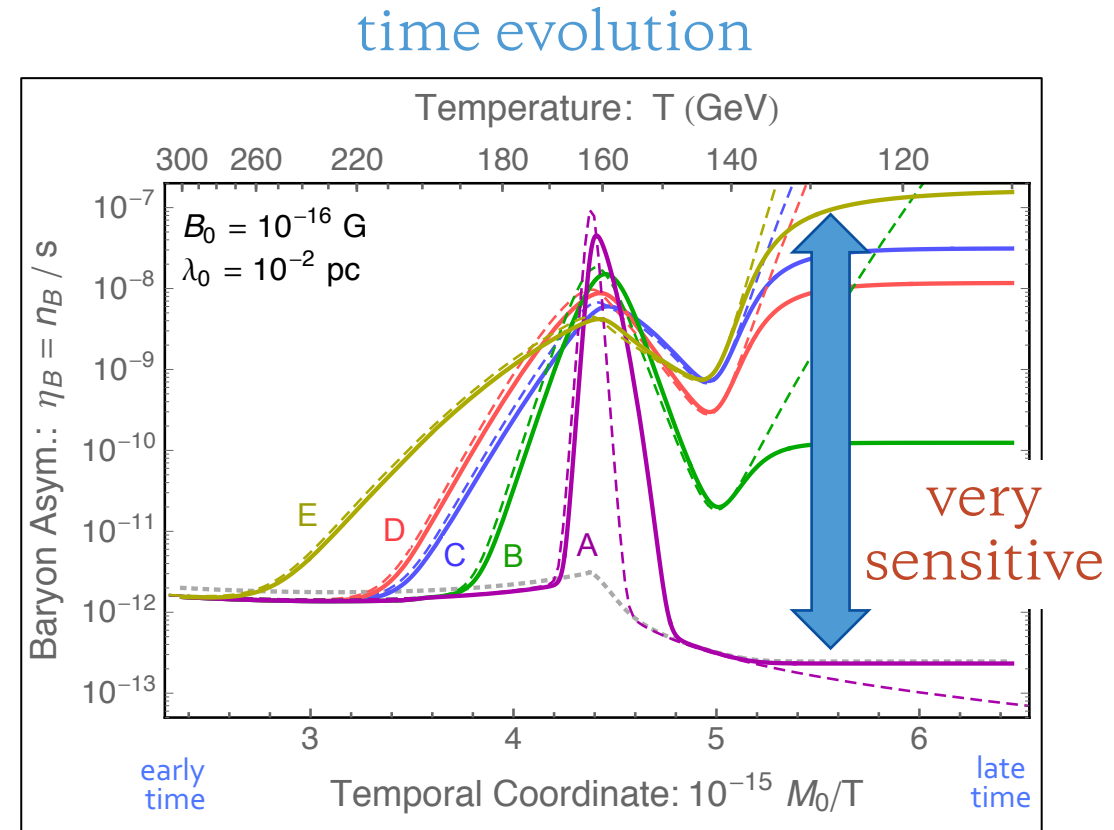
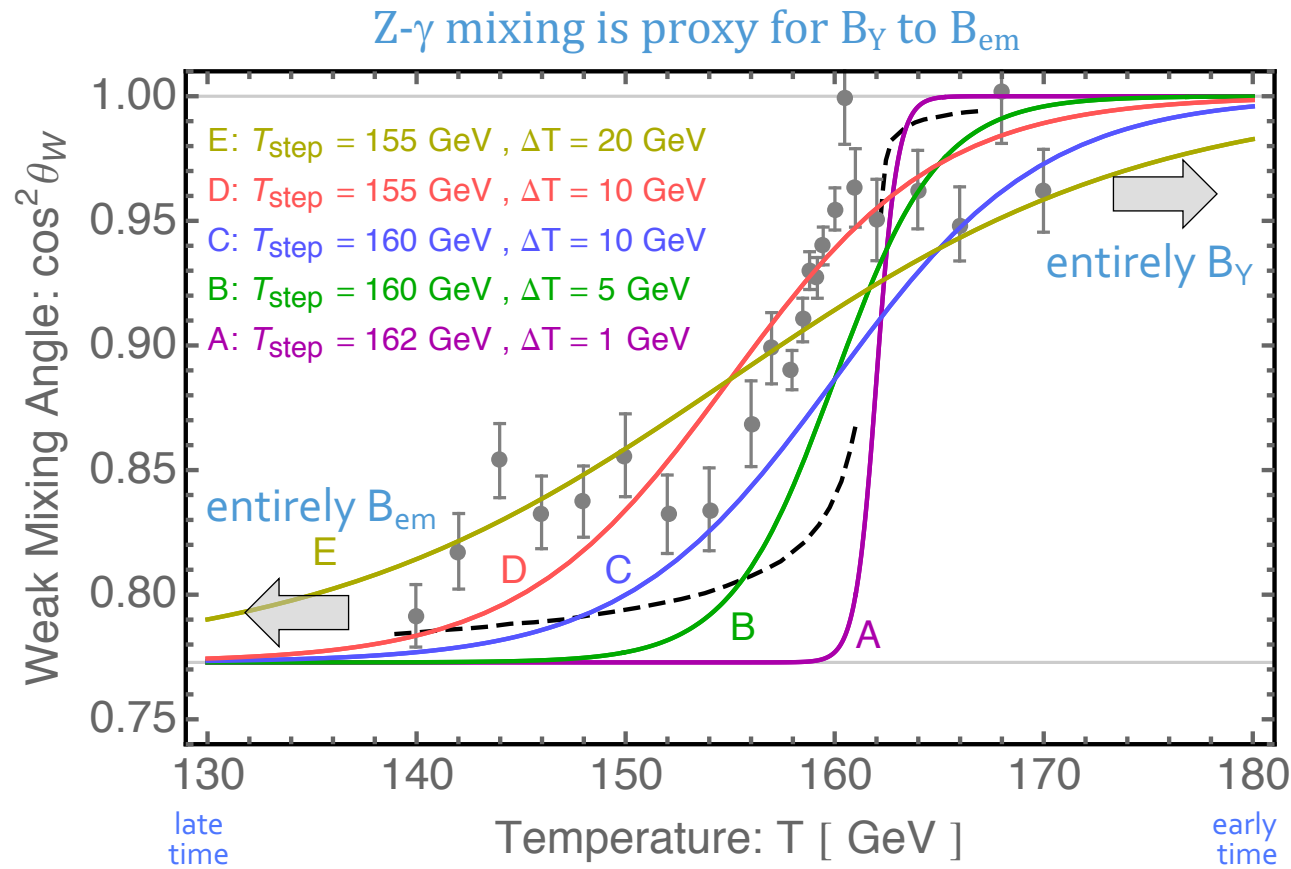
basic idea: $\dot{n}_B = -\Gamma_{\text{sphaleron}} n_B + S_{\text{helicity}} \quad \Rightarrow \quad n_B \sim S_{\text{helicity}} / \Gamma_{\text{sphaleron}}$

time evolution



Sensitivity to the EW crossover

Kamada & AL (2016)



We should work to develop a better understanding of how hypermagnetic fields are converted into electromagnetic fields at the EW epoch (even if it is a smooth crossover)

Avoiding baryon overproduction

[Domcke, Kamada, Mukaida, Schmitz, Yamada (2022)]

If μ_{Y5} is too large, the helical B_Y -field becomes too strong, and B-number is over-produced.

The upper limit is subject to uncertainties associated with modeling $B_Y \rightarrow B_{EM}$ at the EW crossover.

We take $\mu_{Y,5}/T \lesssim 10^{-2}$ as a guide.

recall

$$B_{\text{phys},0} \simeq (6.6 \times 10^{-16} \text{ G}) \left(\frac{|\mu_{Y,5}|/T}{10^{-3}} \right)^{1/3}$$

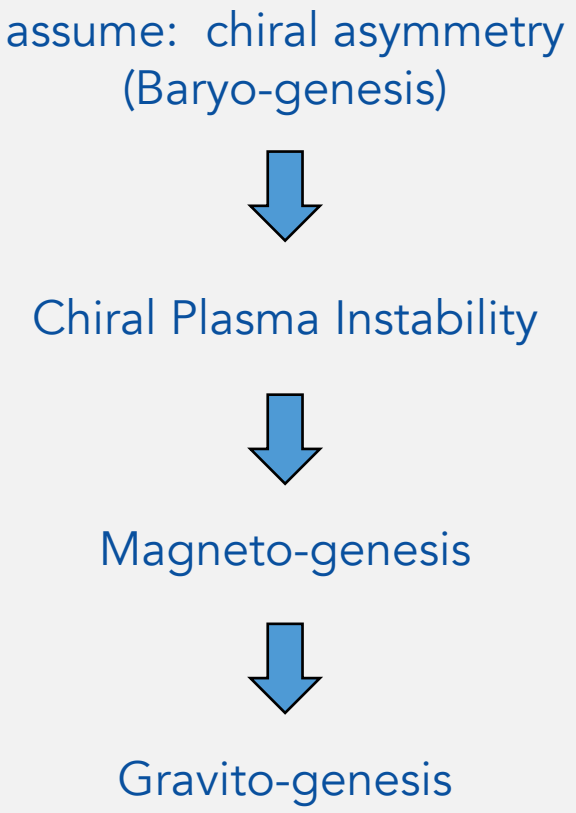
summary graphic
& remarks

Summary

chiral asymmetry
is erased before
magnetogenesis

viable window

baryon number
is over-produced



| | | | |
|--|-----------------------|-----------------------|--|
| | 10^{-3} | 10^{-2} | $(\tilde{\mu}_{Y,5} /T)_{\text{CPI}}$ |
| | 70 TeV | 7000 TeV | $T_{\text{phys,CPI}} \propto (\tilde{\mu}_{Y,5} /T)_{\text{CPI}}^2$ |
| | 7×10^{-16} G | 1×10^{-15} G | $B_{\text{phys},0} \propto (\tilde{\mu}_{Y,5} /T)_{\text{CPI}}^{1/3}$ |
| | 9×10^{-4} pc | 2×10^{-3} pc | $\xi_{M,\text{phys},0} \propto (\tilde{\mu}_{Y,5} /T)_{\text{CPI}}^{1/3}$ |
| | 7×10^{-39} | 7×10^{-33} | $\Omega_{\text{GW}} h_0^2 \propto (\tilde{\mu}_{Y,5} /T)_{\text{CPI}}^6$ |
| | 0.1 MHz | 1 MHz | $f_{\text{GW},0} \propto (\tilde{\mu}_{Y,5} /T)_{\text{CPI}}$ |

- chiral plasma instability develops at $T_{\text{CPI}} > 80$ TeV before washout
- development of CPI leads to helical PMFs and chiral PGWs
- the PMFs survives as an intergalactic magnetic field ~ too weak for blazars
- the PGWs are high frequency ~ too weak for laboratory detection

backup slides



A note on notation

All dimensionful variables are comoving. Some examples,

conformal time:

$$dt = dt_{\text{phys}}/a$$

comoving Hubble param:

$$H = aH_{\text{phys}}$$

comoving temperature:

$$T = aT_{\text{phys}}$$

comoving energy density:

$$\mathcal{E} = a^4 \mathcal{E}_{\text{phys}}$$

comoving chemical potential:

$$\mu = a\mu_{\text{phys}}$$

comoving magnetic field strength:

$$\mathbf{B} = a^2 \mathbf{B}_{\text{phys}}$$

comoving magnetic correlation length:

$$\xi_M = \xi_{M,\text{phys}}/a$$

comoving conductivity:

$$\sigma = a\sigma_{\text{phys}}$$

Friedmann equation:

$$3a^2 M_{\text{pl}}^2 H^2 = \mathcal{E}$$

Stochastic B-field power spectra & energy

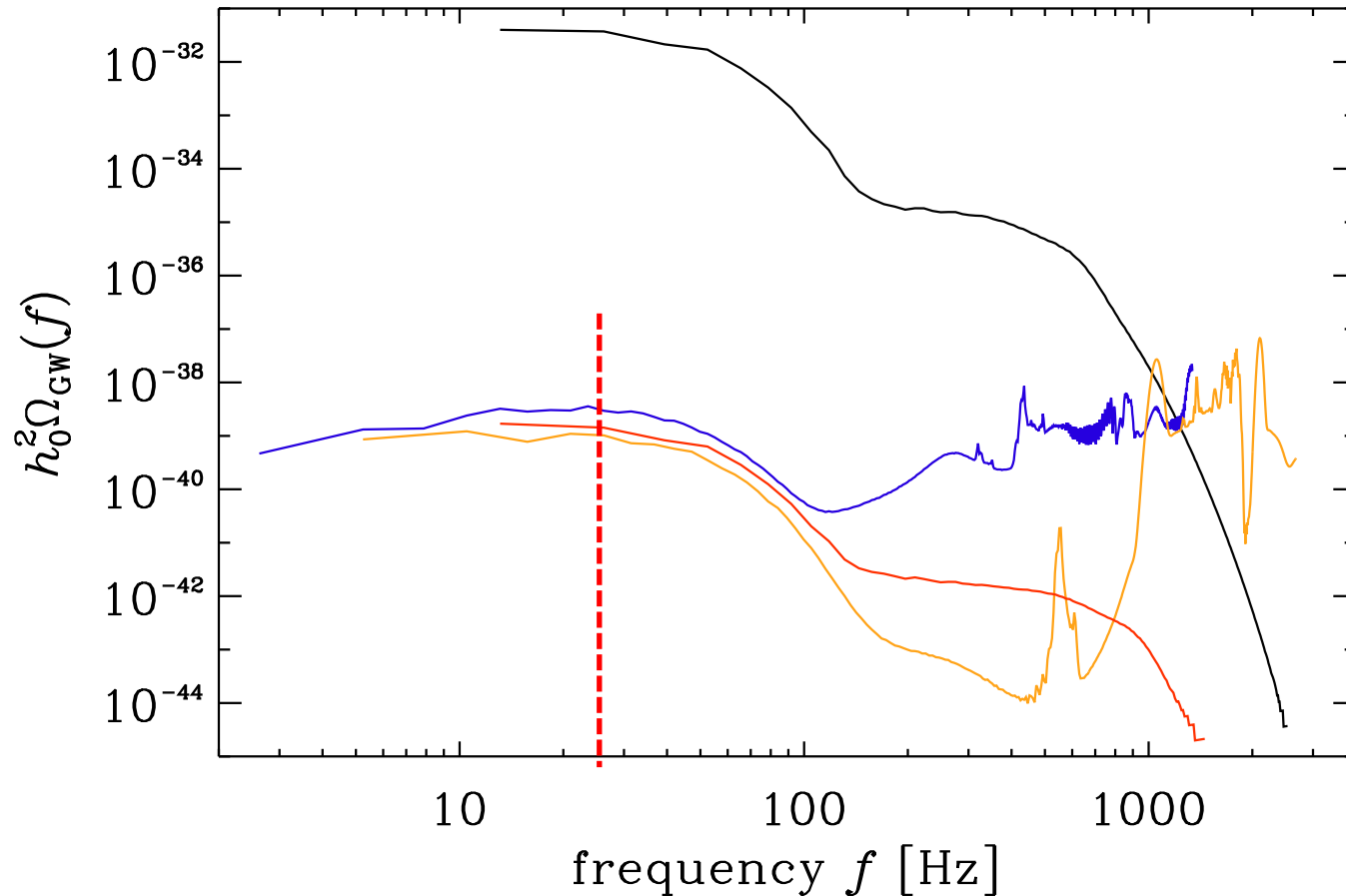
$$\langle B_i(\mathbf{k}, t) B_j^*(\mathbf{k}', t) \rangle = (2\pi)^3 \delta(\mathbf{k} - \mathbf{k}') \left[(\delta_{ij} - \hat{k}_i \hat{k}_j) P_B(k) - i\epsilon_{ijm} \hat{k}_m P_{aB}(k) \right]$$

$$\begin{aligned} \langle B_i(\mathbf{x}, t) B_j(\mathbf{y}, t) \rangle &= \int \frac{d^3 \mathbf{k}}{(2\pi)^3} \frac{d^3 \mathbf{k}'}{(2\pi)^3} \langle B_i(\mathbf{k}, t) B_j^*(\mathbf{k}', t) \rangle e^{i\mathbf{k} \cdot \mathbf{x} - i\mathbf{k}' \cdot \mathbf{y}} \\ &= \int \frac{d^3 \mathbf{k}}{(2\pi)^3} \left[(\delta_{ij} - \hat{k}_i \hat{k}_j) P_B(k) - i\epsilon_{ijm} \hat{k}_m P_{aB}(k) \right] e^{i\mathbf{k} \cdot (\mathbf{x} - \mathbf{y})} \end{aligned}$$

$$\begin{aligned} \mathcal{E}_M(\mathbf{x}, t) &= \frac{1}{2} \sum_i \langle B_i(\mathbf{x}, t) B_i(\mathbf{x}, t) \rangle \\ &= \frac{1}{2} \int \frac{d^3 \mathbf{k}}{(2\pi)^3} \left[(3 - 1) P_B(k) \right] \\ &= \int \frac{d^3 \mathbf{k}}{(2\pi)^3} P_B(k) \\ &= \int_0^\infty \frac{dk}{k} \underbrace{\frac{k^3}{2\pi^2} P_B(k)}_{= k E_M(k)} \end{aligned}$$

Grav wave frequency spectrum today

Run X4: $k_1/H_* = 5 \times 10^3$ Run Y2: $k_1/H_* = 2 \times 10^3$
Run Y3: $k_1/H_* = 10^3$ Run Y1: $k_1/H_* = 5 \times 10^3$

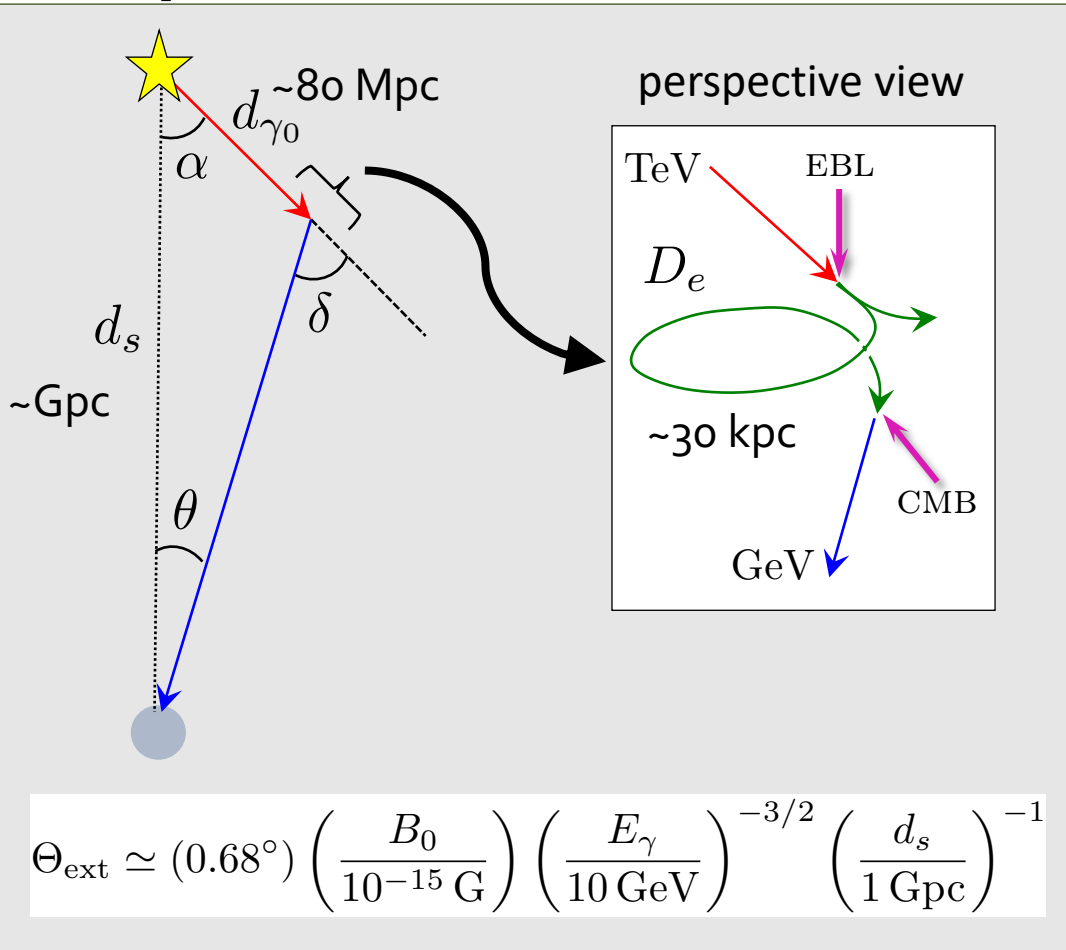


- a high-frequency & low amplitude
- UV end of the spectrum suffers from numerical instability (that depends on the k_1 , highest wavenumber on the lattice)

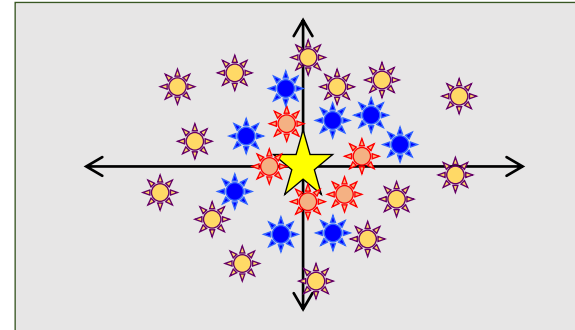
TeV blazars
as a probe of the IGMF

Gamma rays from TeV blazars develop an electromagnetic cascade by scattering on starlight (EBL) and cosmic microwave background (CMB) photons.

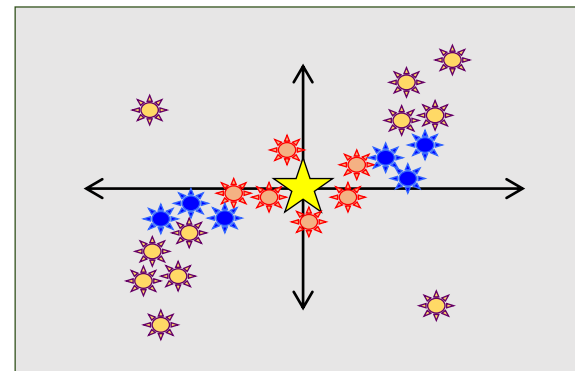
The presence of an IGMF deflects the cascade.



the blazar acquires a halo

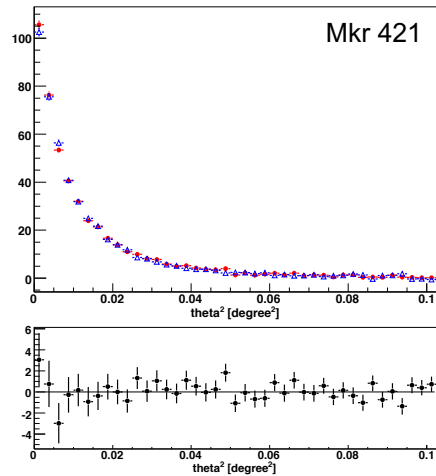


the blazar halo becomes “twisted” by a *helical* IGMF

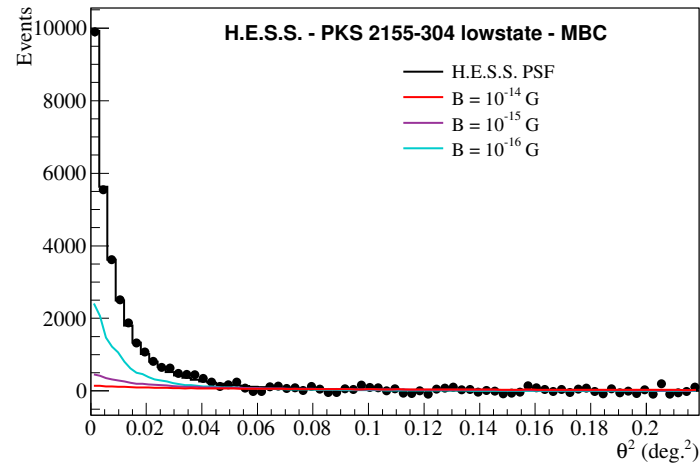


Ongoing experimental efforts ...

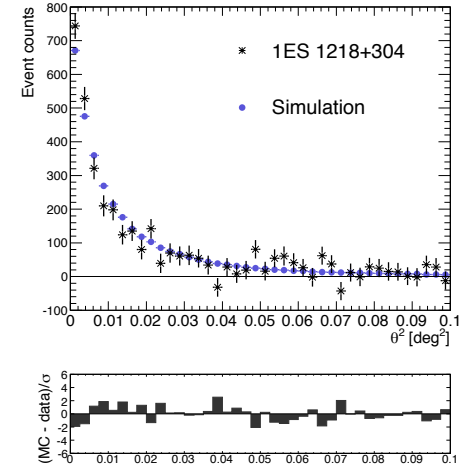
MAGIC (2010)



HESS + Fermi-LAT (2014)



VERITAS (2017)

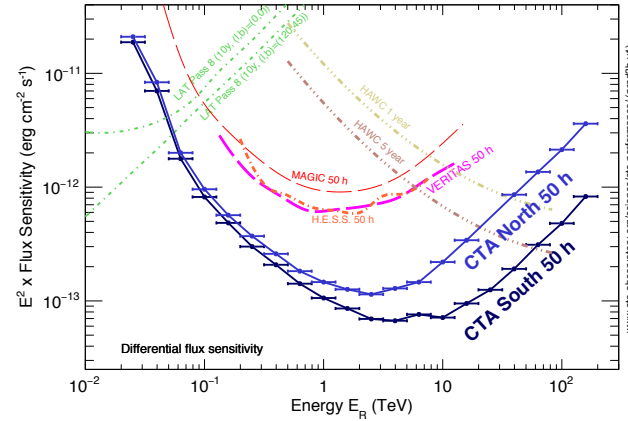


A halo is not observed → some of the IGMF parameter space is excluded:

$$B_0 \sim (0.3 - 70) \times 10^{-15} \text{ G} \quad \text{for} \quad \lambda_0 = 1 \text{ Mpc}$$

On the horizon...

The Cherenkov Telescope Array (CTA) will dramatically improve the flux sensitivity & angular resolution (PSF).



Implications for IGMF constraints:

Benchmark models (3, green). Corresponding exclusions (blue).

